AlGaN–GaN HEMTs on SiC With CW Power Performance of $>$4 W/mm and 23% PAE at 35 GHz

Cathy Lee, Paul Saunier, Jinwei Yang, and M. Asif Khan

***Abstract*—In this letter, continuous wave Ka-band power performance of AlGaN–GaN high electron-mobility transistors grown on semi-insulating SiC substrates are reported. The devices, with gate lengths of 0.25 μm, exhibited maximum drain current density of 1.1 A/mm and peak extrinsic transconductance of 285 mS/mm. At 35 GHz, an output power density of 4.13 W/mm with 23% of power-added efficiency (PAE) and 7.54 dB of linear gain were achieved at a drain bias of 30 V. These power results represent the best power density, PAE, and gain combination reported at this frequency. The drain bias dependence of the Ka-band power performance of these devices is also presented.**

***Index Terms*—AlGaN, GaN, microwave power high electron mobility transistors (HEMTs).**

I. INTRODUCTION

AlGaN–GaN heterostructure field-effect transistors have shown strong potential to be the building blocks of next-generation microwave power amplifiers. Small gate periphery devices grown on SiC substrates have exhibited a power density of 9.8 to 10.7 W/mm at X-band [1], [2], and more recently a total output power of 38 W with 29% power-added efficiency (PAE) was achieved by a 12 mm GaN HEMT hybrid amplifier [3]. Based on these experimental results, for the same output power, the components based on AlGaN–GaN high electron mobility transistors (HEMTs) will benefit greatly from a reduction in matching circuit complexity and chip size, which will lead to lowering of the chip cost. Also, requirements of cooling for high-power transistors are minimized due to the excellent thermal conductivity of SiC substrates.

There is increasing interest to utilize the advantages of AlGaN–GaN HEMTs for high-power applications beyond X-band such as satellite communications and local multipoint distribution systems (LMDS) in Ka-band (26.5–40 GHz). Initial investigations showed pulsed and continuous wave (CW) output power performance in the range of 1.5 W/mm at 29 and 30 GHz [4], [5]. Recently, Kasahara *et al.* reported a CW saturated power density of 6.4 W/mm, a peak PAE of 38%, and a linear gain of 8.8 dB at 30 GHz [6]. High total output power of 0.91 W (1.26 W/mm) with PAE of 10% and 0.62 W (0.86 W/mm) with PAE of 4% were achieved by 0.15-μm gate-length devices at 35 and 40 GHz, respectively [5], [7]. In this letter, we report CW power results of 0.25-μm gate-length AlGaN–GaN HEMTs at both 30 and 35 GHz. While achieving excellent results at 30 GHz, the 200-μm gatewidth device also exhibited a record power density of 4.13 W/mm (0.83 W) at 35 GHz with the best combination of power density, PAE (23%) and linear gain (7.54 dB) to date.

II. DEVICE TECHNOLOGY

The AlGaN–GaN epi layers were grown at the University of South Carolina on a 2 in semi-insulating 4H-SiC substrate by metal organic chemical vapor deposition (MOCVD). The undoped heterostructure consisted of a 200-nm-thick AlN layer, a 2-μm undoped GaN buffer and a 230-Å $Al_{0.25}Ga_{0.75}N$ barrier layer, where trace amounts of Indium were incorporated in all layers to reduce interface roughness. The effect of the presence of low-level flux of trimethyindium (TMI) in the growth of AlGaN–GaN HEMT epi on the reduction of current degradation under pulsed conditions have been published previously in [9]. Kumar *et al.* characterized the improvement in current collapse by first measuring the dc drain current level at zero gate bias on samples grown with TMI flux and without TMI flux. Then, the drain current was measured again on both samples by pulsing the gate bias voltage from the threshold voltage to zero volts of gate bias [9]. Ideally, the devices should have the same amount of current under pulsing conditions, and the ratio of pulsed drain current to dc drain current is desired to be 1. The previous study showed that the samples grown without TMI flux had a pulsed to dc current ratio of 0.45 to 0.7. On the other hand, samples grown with TMI flux had a pulsed to dc current ratio of 0.85 to 1 [9]. Consequently, the devices reported by Kumar *et al.* exhibited high dc and record small-signal high frequency results of f_T and $f_{\max}$, however, large signal power results were not shown. Sheet resistance mapping across the 2 in wafer yielded an average sheet resistance of 325 Ω/sq.

The device fabrication was completed at TriQuint Semiconductor Texas' facility. Each level was patterned using a production I-line stepper, except for gates. Mesa isolation was defined using reactive ion etching (RIE) in a Cl_2/Ar plasma. The source and drain ohmic contacts were formed using an alloyed Ti/Al/Ti/Au metallization. The ohmic contact resistance was 0.57 Ω-mm as measured by the transmission line method. T-shaped 0.25-μm Pt/Au Schottky gates, centered within 4-μm source–drain channel, were fabricated by electron beam lithography. Surface passivation, which is critical in reducing the frequency-dependent current lag phenomenon, was Si_3N_4. Prior to deposition, the wafer was cleaned in solvents and diluted HCl. 1000 Å of Si_3N_4 were deposited by a plasma-enhanced chemical vapor deposition (PECVD)

Manuscript received February 10, 2003; revised July 10, 2003. This work was supported by a grant from the Lockheed Martin Corporation.The review of this letter was arranged by Editor D. Ueda.

C. Lee and P. Saunier are with Research and Development Engineering, TriQuint Semiconductor Texas, Richardson, TX 75083 USA (e-mail: clee@tqtx.com).

J. Yang and M. A. Khan are with the Department of Electrical and Computer Engineering, University of South Carolina, Columbia, SC 29208 USA .

Digital Object Identifier 10.1109/LED.2003.817383

system. Standard gold air-bridge plating process was used for connecting multi-finger devices.

Typical dc transfer characteristics of a 200-μm gatewidth device with gate length $L_G = 0.25$ μm and gate-drain spacing $L_{\mathrm{GD}} = 1.87$ μm are shown in Fig. 1. The peak extrinsic transconductance, g_m, of approximately 285 mS/mm was measured at a gate bias of -2.9 V and at a drain bias of 10 V. High transconductance (>200 mS/mm) is maintained over a broad range of gate bias values of -3.5 to -1 V. The extrapolated threshold voltage was -3.75 V. Typical dc drain current–voltage characteristics are shown in the inset of Fig. 1. The maximum saturation current, $I_{\max}$, at $V_{\mathrm{GS}} = 2$ V was 1.1 A/mm with an I_{dss} of 910 mA/mm. The forward turn-on voltage of the gate-drain diode ranges between 1.9 and 2.0 V and the reverse breakdown voltage was 40 V.

Small-signal s-parameters, measured on-wafer at $V_{\mathrm{DS}} = 10$ V and $V_{\mathrm{GS}} = -3$ V, yielded unity current-gain cutoff frequencies, f_T, of 40 to 44 GHz for various 200-μm gatewidth devices. The average maximum frequency of oscillation $f_{\max}$, determined from the MSG data, was 84 GHz. The peak f_T was measured at a drain current of 235 mA/mm, where maximum g_m occurred. Compared with devices of the same gate-length that we fabricated previously, these devices showed a 20% increase in f_T, which can be correlated directly with 20% higher in measured g_m.

III. LARGE SIGNAL PERFORMANCE

The CW Ka-band power performance was characterized without cooling by on-wafer load-pull at 30 and 35 GHz. A 200-μm device with a 50-μm unit gate width was measured under class AB operation. Fig. 2 shows that at $V_{\mathrm{DS}} = 30$ V and at a quiescent current of 325 mA/mm, output power density of 5.43 W/mm (1.09 W) was achieved at maximum PAE of >33% with a linear gain of 9.17 dB at 30 GHz. Under the same bias, the same device delivered a remarkable P_{out} of 4.13 W/mm (0.83 W) at peak PAE of 23% with a linear gain of 7.54 dB, demonstrating the best power density, PAE, and gain combination at 35 GHz to date. The power gain at peak PAE was compressed by approximately 2 to 6.9 dB at 30 GHz and 5.54 dB at 35 GHz.

The drain-bias dependence of the power performance at Ka-band was investigated at V_{DS} of 15, 20, 25, 30, and 35 V for each frequency, while keeping the current density at 325 mA/mm in all measurements. The data point at 35 V at 35 GHz was excluded due to insufficient input power to saturate the device. Fig. 3 shows the power density and their corresponding peak PAE at each of the experimented bias points at 30 and 35 GHz. At a low bias of 15 V, more than 3 W/mm of power density was measured with a high associated PAE of 44% at 30 GHz. Similarly, the highest maximum PAE of 32% at 35 GHz was obtained at $V_{\mathrm{DS}} = 15$ V with $P_{\mathrm{out}} = 2.84$ W/mm. The results at 35 GHz represent significant improvement in power density and PAE at 15 V over the previously published data. As shown in Fig. 3, the saturated P_{out} increased gradually as a function of V_{DS} to 5.68 W/mm at 35 V and 30 GHz and 4.13 W/mm at 30 V and 35 GHz. As the drain voltage was increased, the available voltage swing was also increased, leading to an initial linear rise in the saturated power at both frequencies. However, the observed nonlinear behavior at higher drain voltages may be explained by heating. The decrease in peak PAE from 44 to 30% at 30 GHz and from 32 to 23% at 35 GHz may be attributed to the increase in radio frequency (RF) knee voltage at high drain bias. The reduction may also be a result of the change in voltage swing as the bias voltage approaches the breakdown voltage. Fig. 4 shows the measured linear gain and power gain at peak PAE as a function of the drain bias. The high linear gain of >9 and 7.5 dB were measured at each frequency, and remained fairly constant as the drain voltage was increased. The power gain increased slightly by 0.7 dB at 30 GHz and by 0.9 dB at 35 GHz, which indicates that f_T and $f_{\max}$ do not degrade as the drain bias is increased from 15 to 35 V of drain bias.

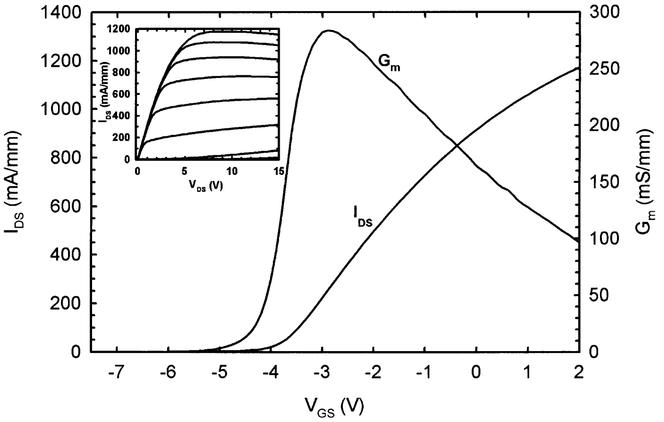

Fig. 1. DC transfer characteristics of a 200-μm AlGaN–GaN HEMT. The drain bias was 10 V. Inset: dc drain current–voltage characteristics where $V_{\mathrm{GS}} = 2$ to -5 V.

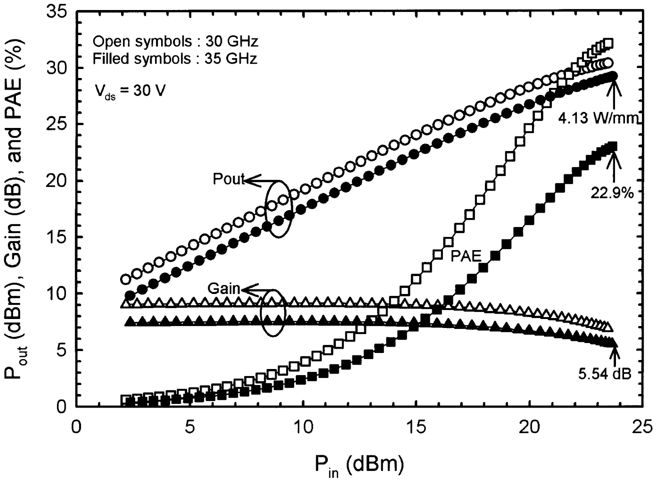

Fig. 2. Output power, PAE, and gain as a function of input power of a 200-μm AlGaN–GaN HEMT at 30 and 35 GHz. $V_{\mathrm{DS}} = 30$ V at both frequencies.

IV. CONCLUSION

In summary, we have reported CW power results at Ka-band on 0.25-μm AlGaN–GaN HEMTs grown on SiC. The devices showed dc maximum drain current of 1.1 A/mm with peak transconductance of 285 mS/mm. Small signal characterization

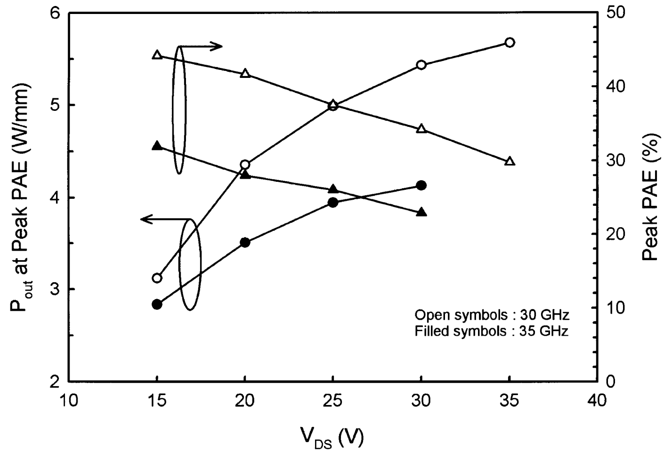

Fig. 3. Output power density at peak PAE and maximum PAE as a function of drain bias measured at 30 and 35 GHz of a 200-μm AlGaN–GaN HEMT.

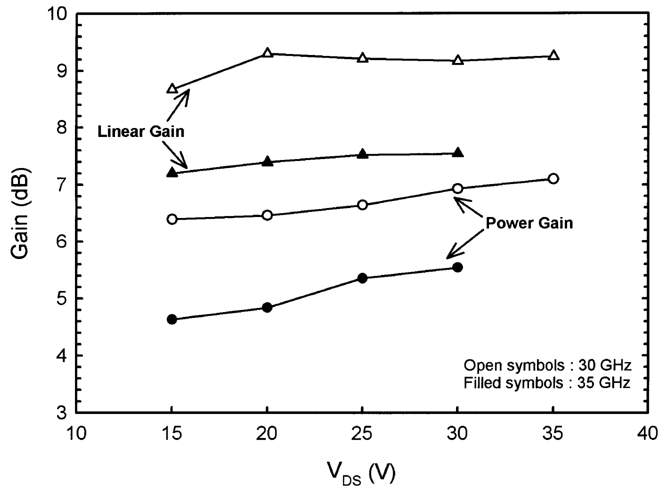

Fig. 4. Linear gain and power gain as a function of drain bias measured at 30 and 35 GHz of a 200-μm AlGaN–GaN HEMT.

showed f_T and $f_{\max}$ of 40 and 84 GHz, respectively. At 30 GHz, output power density of 5.68 W/mm at $V_{\rm DS} = 35$ V and a high PAE of 44% at $V_{\rm DS} = 15$ V were achieved. At 35 GHz, a power density of 4.13 W/mm (0.83 W) was delivered by a 200-μm gatewidth device with 23% of PAE and 7.54 dB of linear gain, representing a breakthrough power density achieved by a single device at this frequency. With further optimization in device design, better performance can be expected from AlGaN–GaN HEMTs for high-power applications in Ka-band.

ACKNOWLEDGMENT

The authors would like to thank G. Oliver and H. Gerring for the processing assistance and L. Gooch for the load–pull measurements. Also, the encouragement and support from D. C. Dumka, M. Muir, and H. Q. Tserng are appreciated.

REFERENCES

[1] Y.-F. Wu, D. Kapolnek, J. P. Ibbetson, P. Parikh, B. P. Keller, and U. K. Mishra, “Very-high power density AlGaN–GaN HEMTs,” *IEEE Trans. Electron Devices*, vol. 48, pp. 586–590, Mar. 2001.

[2] V. Tilak, B. Green, V. Kaper, H. Kim, T. Prunty, J. Smart, J. Shealy, and L. Eastman, “Influence of barrier thickness on the high-power performance of AlGaN–GaN HEMTs,” *IEEE Electron Device Lett.*, vol. 22, pp. 268–270, Nov. 2001.

[3] W. L. Pribble, J. W. Palmour, S. T. Sheppard, R. P. Smith, S. T. Allen, T. J. Smith, Z. Ring, J. J. Sumakeris, A. W. Saxler, and J. W. Milligan, “Applications of SiC MESFETs and GaN HEMTs in power amplifer design,” in *Proc. IEEE MTT-S Microwave Symp.*, 2002, pp. 1819–1822. Seattle.

[4] R. Sandhu, M. Wojtowicz, M. Barsky, R. Tsai, I. Smorchkova, C. Namba, P. H. Liu, R. Dia, M. Truong, D. Ko, J. W. Yang, H. Wang, and M. A. Khan, “1.6 W/mm, 26% PAE AlGaN–GaN HEMT operation at 29 GHz,” in *IEDM Tech. Dig.*, Washington, DC, 2001, pp. 940–942.

[5] R. Kiefer, R. Quay, S. Muller, K. Kohler, F. V. Raay, B. Raynor, W. Pletschen, H. Massler, S. Ramberger, M. Mikulla, and G. Weimann, “AlGaN–GaN-HEMTs for power applications up to 40 GHz,” in *Proc. IEEE Eastman Conf. High-Performance Devices*, Newark, NJ, Aug. 2002, pp. 502–504.

[6] K. Kasahara, H. Miyamoto, Y. Ando, Y. Okamoto, T. Nakayama, and M. Kuzuhara, “Ka-band 2.3 W power AlGaN–GaN heterojunction FET,” in *IEDM Tech. Dig.*, San Francisco, CA, Dec. 2002, pp. 677–680.

[7] R. Quay, R. Kiefer, F. van Raay, H. Massler, S. Ramberger, S. Muller, M. Dammann, M. Mikulla, M. Schlechtweg, and G. Weimann, “AlGaN–GaN HEMTs on SiC operating at 40 GHz,” in *IEDM Tech. Dig.*, San Francisco, CA, Dec. 2002, pp. 673–676.

[8] M. A. Khan, X. Hu, A. Tarakji, G. Simin, J. Yang, R. Gaska, and M. S. Shur, “AlGaN–GaN metal–oxide–semiconductor heterostructure field-effect transistors on SiC substrates,” *Appl. Phys. Lett.*, vol. 77, pp. 1339–1341, Aug. 2000.

[9] V. Kumar, W. Lu, R. Schwindt, A. Kuliev, G. Simin, J. Yang, M. A. Khan, and I. Adesida, “AlGaN–GaN HEMTs on SiC with f_T over 120 GHz,” *IEEE Electron Device Lett.*, vol. 23, pp. 255–257, Aug. 2002.

[10] C. Lee, H. Wang, J. Yang, L. Witkowski, M. Muir, M. A. Khan, and P. Saunier, “State-of-art CW power density achieved at 26 GHz by AlGaN–GaN HEMTs,” *Electron. Lett.*, vol. 38, pp. 924–925, Aug. 2002.